ELSEVIER

Journal of Fluids and Structures 21 (2005) 75–87

JOURNAL OF FLUIDS AND STRUCTURES

www.elsevier.com/locate/jfs

Fluidelastic instability tests on an array of tubes preferentially flexible in the flow direction

N.W. Mureithi*, C. Zhang, M. Ruël, M.J. Pettigrew

BWC/AECL/NSERC Chair of Fluid-Structure Interaction, Department of Mechanical Engineering, École Polytechnique de Montréal, Montréal, QC, Canada, H3T 1J4

Received 1 October 2004; accepted 18 March 2005

Abstract

The present work is motivated by the observation that, in the presence of flat bar supports (AVBs), U-tubes in steam generators and heat exchangers may not be restrained in the in-plane direction. The stability behavior of a rotated triangular array is investigated in detail in the present work. Tests are conducted with a fully flexible array, a single flexible tube, and a finite number of flexible tubes at several locations within the otherwise rigid array. In all cases tube flexibility is purely in the flow direction. The fully flexible array is shown to undergo fluidelastic instability. Despite the unidirectional flexibility constraint, the critical instability velocity is of the same order of magnitude when compared with previous tests on an unconstrained fully flexible array. A single flexible tube, on the other hand, is found to be stable. Results of tests on partially flexible array configurations are also presented.

Keywords: Tubes preferentially flexible; Rotated triangular array; Fluidelastic instability

1. Introduction

Fluidelastic instability remains a concern in the design of shell-and-tube heat exchangers and nuclear steam generators. The reviews of Paidoussis (1983), Weaver and Fitzpatrick (1988), Pettigrew and Taylor (1991) and Price (1995) trace the discovery of fluidelastic instability, initial attempts to understand this phenomenon and the development of theoretical models to explain and predict fluidelastic instability. Mechanisms underlying fluidelastic instability were elucidated in the theoretical work of Chen (1983). Pettigrew and Taylor (1994) trace the development of work on fluidelastic instability in two-phase flows, an area where many unanswered questions remain. The authors have also recently presented an updated review and design guidelines in Pettigrew and Taylor (2003). The region of concern in Steam Generators (SG) is the upper most U-bend region. The large radius outer tubes can undergo fluidelastic instability if not sufficiently supported. Tube support is usually provided by flat bars or Anti-Vibration Bars (AVBs) inserted radially outward between tube rows.

A large body of work exists on fluidelastic instability of tube arrays in cross-flow. Numerous tests on axisymmetrically flexible tube bundles show that instability is often in the transverse direction. This is the case of out-of-plane instability in the U-bend region.

*Corresponding author.
E-mail address: njuki.mureithi@polymtl.ca (N.W. Mureithi).

0889-9746/$ - see front matter
doi:10.1016/j.jfluidstructs.2005.03.010

Contrary to the transverse direction instability, the possibility of instability in the flow direction (in-plane instability) has raised less concern. The in-plane modes have higher frequencies than their out-of-plane counterparts, and correspondingly higher instability velocities. Also many of the reported cases of fluidelastic instability involve purely transverse tube motion or at least coupled transverse/inflow motion, and much less frequently purely inflow instability.

Tests with tubes flexible only in the transverse direction have been reported. Indeed, it is partly as a result of the observation of this out-of-plane instability that improved AVB supporting was introduced in modern SG designs. Weaver and Schneider (1983) reported on the effect of flat bar supports on tube stability in the U-bend region. Supports with small clearances were found to be effective in stabilizing both the out-of-plane and in-plane tube modes. The mechanism by which the in-plane modes were stabilized was, however, not clearly elucidated. Tests were also conducted with scallop supports as well as other support configurations. Significant in-plane vibration was found in the case of scallop bar supports. Due to the nominal clearance of 0.51 mm for these supports, both in-plane and out-of-plane vibrations occurred.

Experimental work to simulate the effect of asymmetric stiffness was also reported by Weaver and Koroyannakis (1983). Differences between streamwise and transverse tube natural frequencies between 6% and 57% were tested. Critical flow velocities were found to increase by up to about 20% relative to the case of symmetrically flexible tubes.

The work reported here pertains to the question of fluidelastic instability in arrays solely flexible in the flow direction. The research is motivated by the need to quantify the risk of in-plane instability in steam generator designs. Flat-bar (AVB) supports in the U-bend region may be considered effective in the out-of-plane direction, even in the presence of small gaps; nonlinear tube/support interaction (impacting) introduces additional damping, while tube/support contact increases the effective stiffness. However, small tube/support gaps render the tube unsupported within the plane, potentially allowing the possibility of significant in-plane vibration due to reduced effective in-plane frequency. Consider a clamped semi-circular tube as an approximation of the U-bend portion of a SG tube. Typical SG tube parameter values may be found in Fluit and Pettigrew (2001). Taking the typical values: U-bend radius $R = 2\,\mathrm{m}$, diameter, $d = 16\,\mathrm{mm}$, wall thickness, $t = 1\,\mathrm{mm}$, density, $\rho = 8000\,\mathrm{kg/m^3}$, and modulus of elasticity, $E = 1.8 \times 10^5\,\mathrm{MPa}$, the in-plane first-mode frequency of the tube without intermediate supports is approximately 3.8 Hz. With a pinned support at its mid-point, the out-of-plane first mode frequency is 4.5 Hz, while the in-plane frequency is essentially unchanged. Additional 'loose' supports would raise the out-plane frequency while the in-plane frequency would remain unchanged.

The tests in air-flow presented here are exploratory tests to investigate instability in the flow direction. It is clear that, in order to arrive at final conclusions regarding stability behavior in actual steam generators, two-phase flow tests are required. A test program using two-phase flow is now in progress. Preliminary results of this work are briefly summarized in Section 3.5 of the paper.

2. Experimental apparatus and test procedure

Experiments were conducted in a wind tunnel with a 305 mm × 305 mm test section, in which the maximum flow velocity $U_{\max}$ is 48.8 m/s in the empty test section, and 8 m/s with the array in place. The tube bundle, shown in Fig. 1,

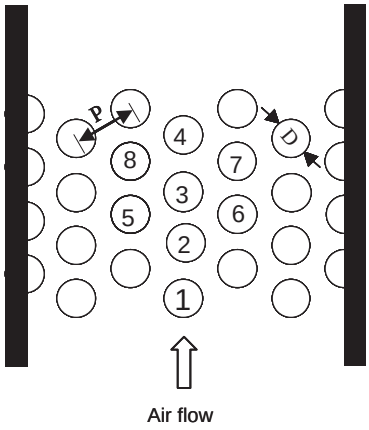

Fig. 1. The rotated triangle test array.

consisted of an array of light-weight tubes with an outside diameter of 40.4 mm, and a height of 270 mm, which was rotated triangular with a pitch ratio $P/D = 1.37$. There were eight rows, with alternately three or two and two-half tubes per row, which provided a uniform flow profile. Each cylinder consisted of a tube with a mild steel thin plate fixed in the middle via a wooden plug. The mild steel thin plate had a 1.5 mm × 15 mm rectangular section, so that vibration was constrained to only one direction. All the tubes were originally designed as cantilever tubes. For the purposes of this study, each tube could be independently restrained from vibrating by means of a rubber stopper inserted in the gap between the tube and the upper test-section window, hence simulating a rigidly fixed tube. Five series of tests were performed in this study. The first test was for one flexible tube, which was located in the second row and middle column. The second test was for two flexible tubes. In this case, the test included two different kinds of configuration, one with two tubes located, respectively, in the third and fifth rows, within the middle column, another with two tubes located, respectively, in the fifth row within the middle column and the fourth row within the neighboring column. The third test was for one column of flexible tubes, which was the middle column with four tubes. The fourth test was for seven flexible tubes, the 'classical' unit that has been sighted as the minimal unit (or kernel) required to model a fully flexible tube bundle. In the fifth test all tubes in the array were flexible.

Before the tube bundle was inserted into the wind tunnel test-section, the static strain-displacement relation for every instrumented tube was determined via a careful calibration. Prior to the wind tunnel tests, the frequency and damping of each of the instrumented tubes were measured by using the logarithmic decrement technique. The data are summarized in Table 1. Each damping value given in the table is the average from at least three different tests. The average tube natural frequency and damping were, 18.74 Hz and 0.44%, respectively. The natural frequency was 188 Hz in the transverse direction, making the tube essentially rigid in this direction. The mass-damping parameter for the test tubes was in the range $2.2 \leqslant m\delta/\rho D^2 \leqslant 3.6$. Note that this falls within the range of typical mass-damping parameter values for steam-generator tubes under prototypical two-phase flow conditions.

In addition to the vibration measurement, the upstream velocity was measured using a Validyne Ultra Low Range Wet–Wet Differential Pressure Transducer model DP103 coupled to a CD23 Digital Transducer Indicator. The velocity was deduced from the measured pressure drop according to the Bernoulli equation. The uncertainty in velocity measurement is approximately ± 0.025 m/s.

Eight tubes were instrumented for vibration monitoring; these tubes are labelled 1–8 in Fig. 1.

The displacement signals of tube vibration were routinely analyzed on an OROS38 8-32 channel real-time multi-analyzer/recorder coupled to a microcomputer. A sampling rate of 1 kHz was chosen. The resulting frequency resolution and frequency range were more than adequate for an average tube frequency of 18.74 Hz. For each test run, sufficient time was allowed for a steady state to be attained (usually several minutes). The flow velocity was recorded and r.m.s displacements determined. Several minutes of raw data for up to eight channels were also recorded for post-processing. The flow velocity was then incremented and the process repeated until the bundle was well into the unstable regime.

3. Results

3.1. Stability behavior of the fully flexible bundle and fixed bundle with a flexible column

Eight tubes (labelled 1–8 in Fig. 1) within the fully flexible bundle were instrumented and monitored tests. The vibration response spectra for the second row tube are shown in Fig. 2. The response spectra show that for low flow velocities, there is minimal excitation due to turbulence. At pitch velocity $U_P = 6.44$ m/s, a strong instability developed. The r.m.s. response amplitude variation with flow velocity is shown in Fig. 3. Increasing the flow velocity to 7.0 m/s resulted in instantaneous peak amplitudes of the order of the inter-cylinder gap. Coincidentally with the large increase in vibration amplitude, a coalescence of the individual tube frequencies to a single modal frequency was observed in Fig. 4, confirming again the onset of fluidelastic instability. Fig. 5 shows the post-instability inter-tube phase

Table 1
Natural frequency and damping for the eight instrumented tubes

	Tube 1	Tube 2	Tube 3	Tube 4	Tube 5	Tube 6	Tube 7	Tube 8	Average
f_n (Hz)	18.89	18.73	18.41	19.05	19.12	18.41	18.57	18.75	18.74
ζ (%)	0.55	0.28	0.46	0.50	0.44	0.57	0.35	0.37	0.44

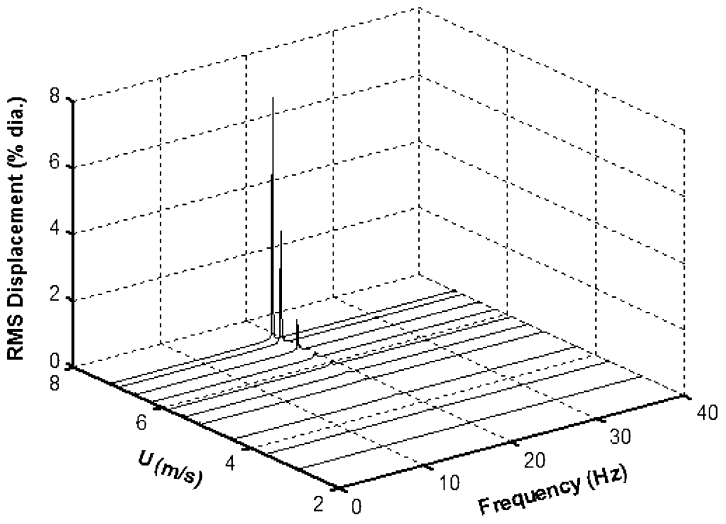

Fig. 2. Response spectra variation with flow velocity for tube 2 in a fully flexible bundle.

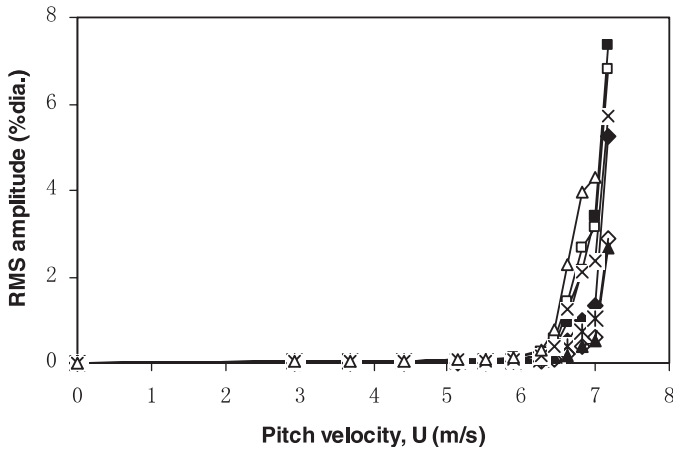

Fig. 3. R.m.s. vibration response for the flexible bundle: ♦, tube 1; ■, tube 2; ∗, tube 3; ▲, tube 4; ◇, tube 5; □, tube 6; ×, tube 7; △, tube 8.

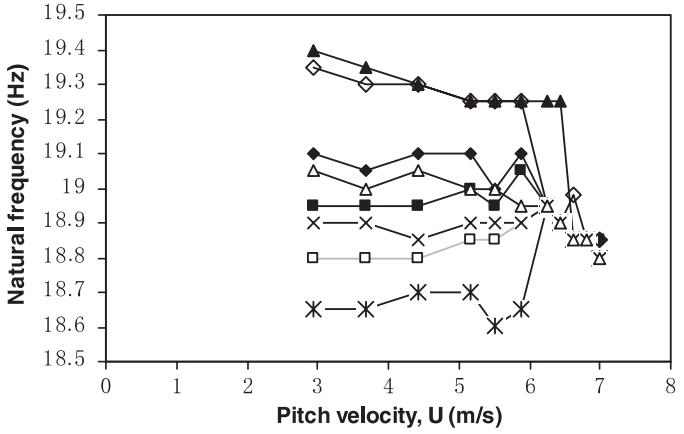

Fig. 4. Response frequency versus flow velocity for the flexible bundle: ♦, tube 1; ■, tube 2; ∗, tube 3; ▲, tube 4; ◇, tube 5; □, tube 6; ×, tube 7; △, tube 8.

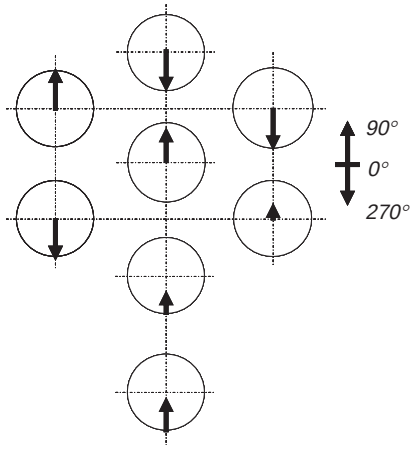

Fig. 5. The unstable mode for the fully flexible bundle; only the instrumented tubes are shown.

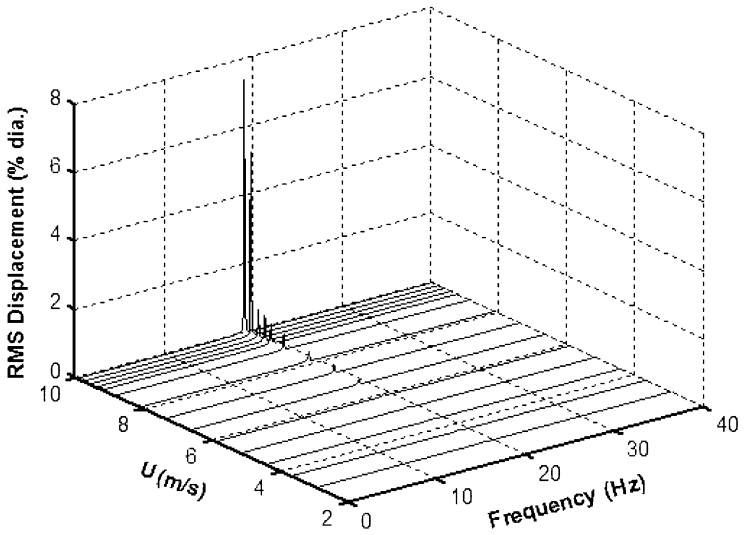

Fig. 6. Response spectra variation with flow velocity for tube 2 located in a flexible tube column.

relationship. In this figure the tube motion is normalized so that the arrow indicates the tube direction of motion. The tip of the arrow marks the position of the tube relative to its equilibrium position. The inter-tube phase relation is the average value over a large number of cycles. There is significant asymmetry in this averaged mode shape. Note, however, that the four downstream tubes (3,4,7 and 8) appear to be highly synchronized. Fig. 5 suggests that a larger number of tubes (possibly the whole array) need to be monitored in order to arrive at a coherent picture of the bundle scale modal pattern. It is suspected, however, that bundle geometry imperfections also introduced some added complexity in the vibration mode exhibited.

In the second series of tests the tubes were fixed leaving only a single flexible column (tubes 1–4) in Fig. 1. The power spectra of the response are shown in Fig. 6. The onset of fluidelastic instability is clearly defined. The amplitude plot of Fig. 7 shows that the critical flow velocity is 9.57 m/s, which is higher than the value of 6.44 m/s obtained for the fully flexible bundle. In Fig. 8 convergence to a single frequency for the tube column at instability is clearly visible. Fig. 9 shows the post-instability phase relationship between the tubes. The latter attain maximum amplitude sequentially, starting with the most downstream tube (tube 4) and ending with tube 1. This suggests a travelling wave phenomenon, travelling in the upstream direction against the flow. Similarly well-defined wave phenomena could not be identified in the case of the fully flexible array, partly due to the limited number of tubes monitored.

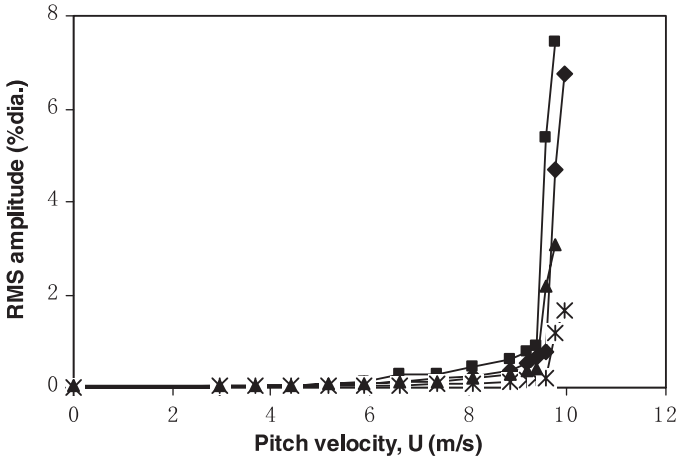

Fig. 7. R.m.s vibration response for the flexible column: ♦, tube 1; ■, tube 2; ∗, tube 3; ▲, tube 4.

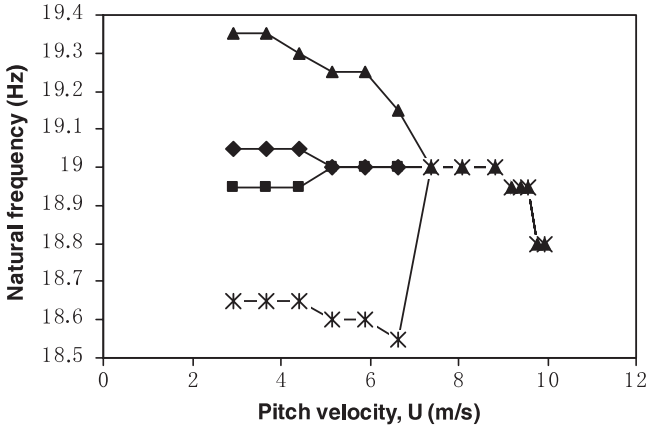

Fig. 8. Response frequency versus flow velocity for the flexible column: ♦, tube 1; ■, tube 2; ∗, tube 3; ▲, tube 4.

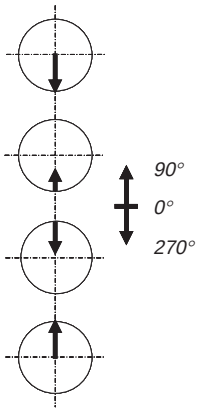

Fig. 9. The unstable mode for the central flexible column tests.

3.2. Stability behavior for two flexible cylinders

The case of a drastically reduced number of flexible tubes is discussed next. The stability behavior changes significantly in the extreme cases of two and then one flexible cylinder. Fluidelastic instability is still manifested for two flexible cylinders. Fig. 10 shows response spectra for a test where tubes 2 and 3 on the middle column are flexible. The spectra shown are those of tube 2. Although the response amplitudes are slightly lower compared to the more flexible arrays, fluidelastic instability clearly occurs. This conclusion is supported by the amplitude and frequency trends in Figs. 11 and 12, respectively. As shown in Fig. 11, instability occurs at a velocity significantly higher than the one for the more flexible configuration. The critical velocity of 13.99 m/s is more than double the critical velocity for the fully flexible array of 6.44 m/s, and about 1.5 times the critical velocity for the single flexible column array of 9.57 m/s, respectively. The instability mechanism is, however, the same yielding a gradual decrease in vibration frequency above the critical velocity. In the case of two flexible cylinders, the relative position of the tubes is crucially important. Fig. 13 shows the vibration response when the two flexible tubes are in neighboring columns; in this case, tubes 3 and 6 were tested. The instability velocity of 16 m/s is higher than that for two tubes in the same column (Fig. 11). The onset of instability is also less abrupt. Furthermore, in Fig. 13 the instability seems to fizzle out for velocities above 18 m/s. This

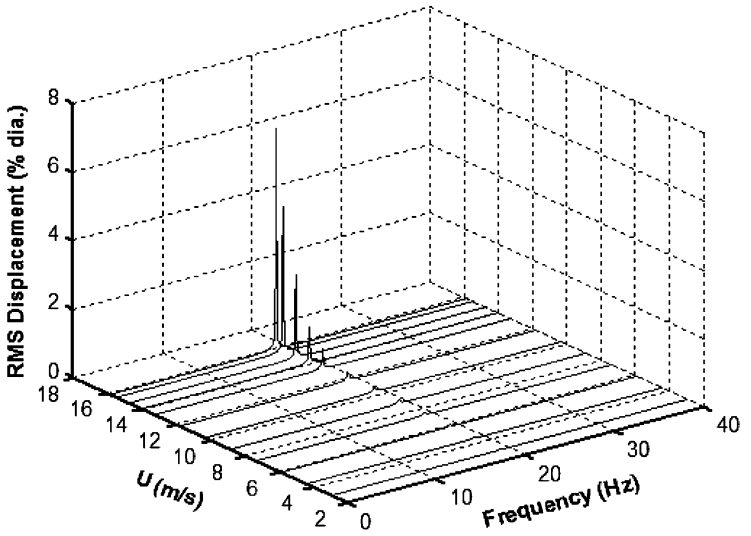

Fig. 10. Response spectra variation with flow velocity for tube 2 for two-flexible cylinder tests.

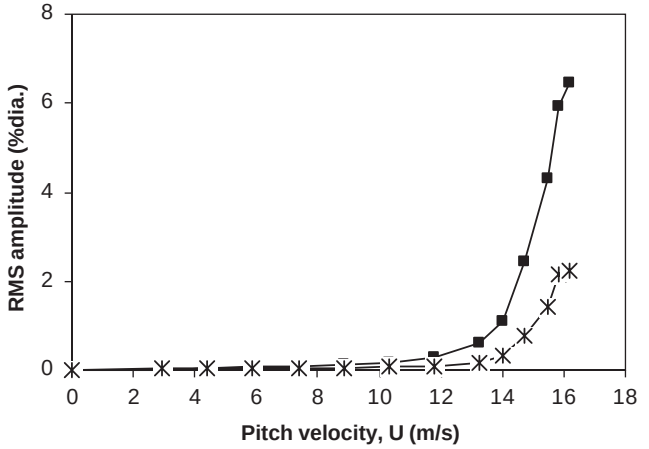

Fig. 11. R.m.s. vibration response for two-flexible tube tests: ■, tube 2; ∗, tube 3.

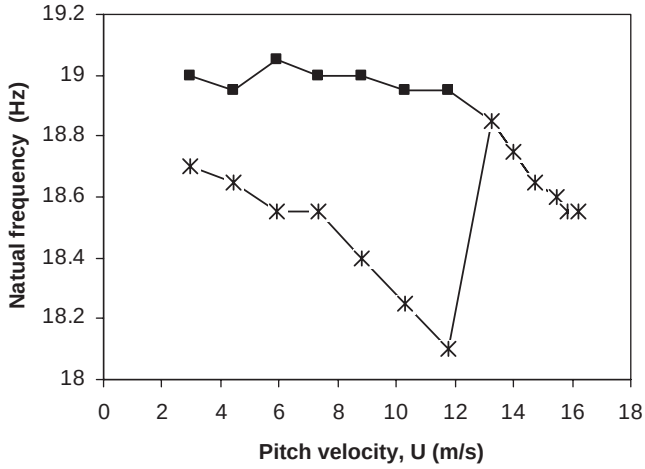

Fig. 12. Response frequency versus flow velocity for two-flexible tube tests: ■, tube 2; ∗, tube 3.

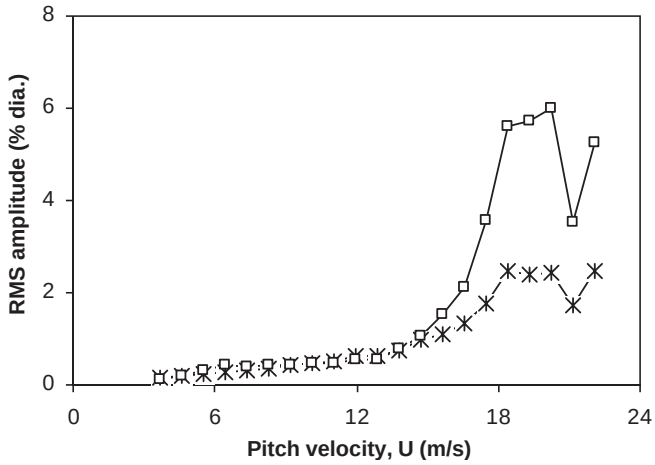

Fig. 13. R.m.s. vibration response for two-flexible tube tests: ∗, tube 3; □, tube 6.

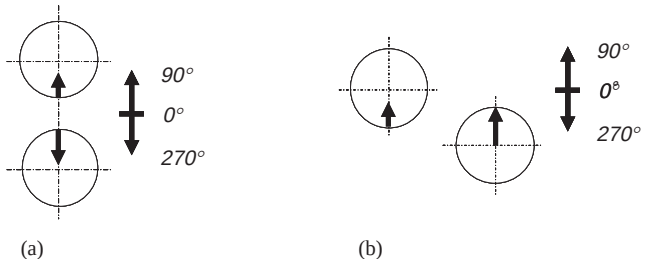

Fig. 14. The unstable modes for two-flexible tube tests: (a) tubes 2 and 3; (b) tubes 3 and 6.

may be due to the steady drag effect, which displaces the tubes from their equilibrium position thus disturbing the array geometry. Fig. 14 shows the post-instability phase relationship between the tubes. In both cases the phase difference is not a rational multiple of the oscillation period. Tubes (2 and 3) in the same column are, however, more clearly out of phase. Furthermore their phase relationship is identical to the case where they form part of the flexible tube column in Fig. 9.

3.3. Dynamics of a single flexible cylinder

One of the most significant sets of test results is for a single flexible cylinder within an otherwise rigid array. The test results are again presented in the same format. Tube 2 was the single flexible tube in the bundle. As shown in the 3-D response spectral plot, Fig. 15, fluidelastic instability did not materialize in this case. Vibration amplitudes (r.m.s.) remained below 0.4% of the tube diameter compared to values as high as 8% of the diameter for the fully flexible array. The amplitude versus pitch velocity plot of Fig. 16 confirms the conclusion of lack of fluidelastic instability. In the frequency plot, Fig. 17, the tube vibration frequency is seen to decrease significantly. However, the maximum flow velocity tested here was much higher than in the other tests. Visual observation of the test cylinder showed that the cylinder suffered a static deflection due to steady drag at the higher velocity. Besides this steady drag effect, no dynamic effect was observed.

3.4. Stability behavior of the seven-tube kernel

The seven-tube kernel is the 'classical' unit that has been sighted as the minimal unit required to model a fully flexible tube bundle. Fig. 18 shows the vibration response for the seven-tube kernel while frequency variation is shown in

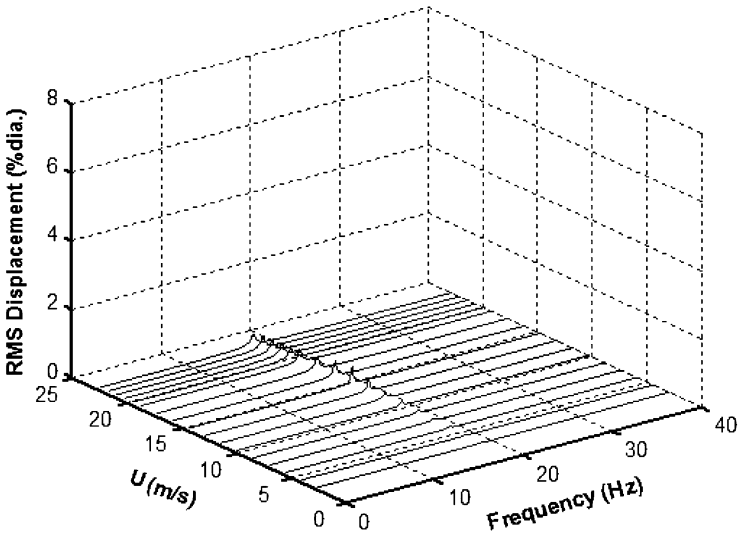

Fig. 15. Response spectra of the single flexible tube (tube 2) in an otherwise rigid bundle.

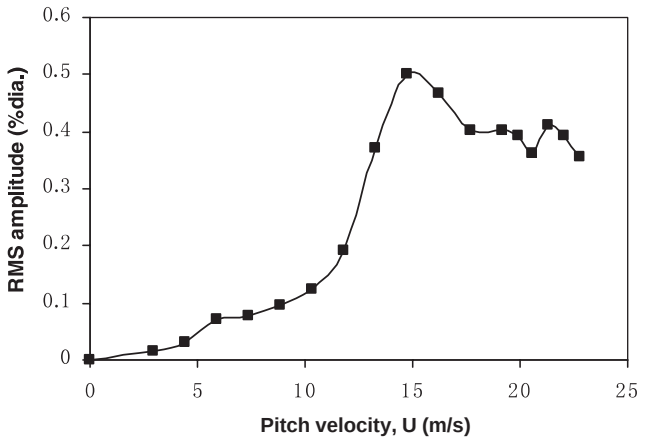

Fig. 16. Vibration amplitudes for a single flexible tube within an otherwise rigid array; ■, tube 2.

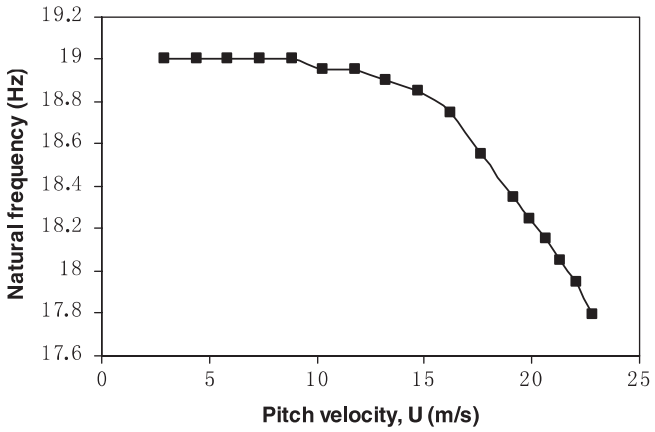

Fig. 17. Response frequency versus flow velocity for single-flexible tube test: ■, tube 2.

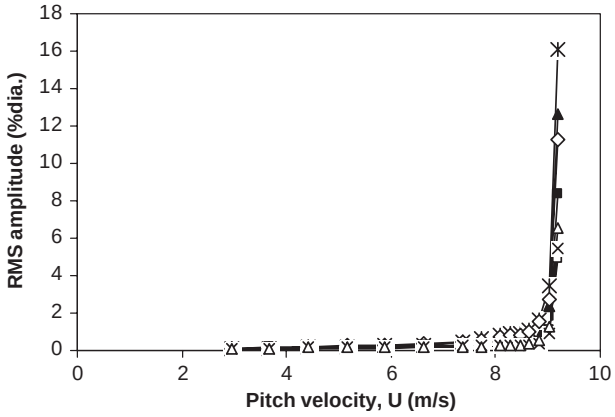

Fig. 18. R.m.s. vibration response for seven-flexible tube test: ■, tube 2; ∗, tube 3; ▲, tube 4; ◇, tube 5; □, tube 6; ×, tube 7; △, tube 8.

Fig. 19. The most remarkable result is the increased stability ($U_{pc} = 9.0\,\mathrm{m/s}$) relative to the flexible bundle which has a critical velocity of 6.44 m/s. The seven-tube kernel is only slightly less stable than the flexible four-tube central column which destabilizes at 9.57 m/s (Fig. 7). Fig. 20 shows the post-instability phase relationship between the tubes. This mode pattern can be compared to the flexible array case shown in Fig. 5; in both cases, the reference tube (4) is at its furthest point upstream (270° phase). The relative motion between tube 4 and its neighbors is completely different in the two cases, indicating that the unstable modes are vastly different.

This result points to the importance of kernel selection when modelling a complete bundle. It is evident that for the present array, which has only unidirectional flexibility, the seven-tube kernel will not be a faithful approximation of fully flexible bundle dynamics. For the rotated triangle array, it is clear that the elimination of bundle flexibility in the direction transverse to the flow greatly affects the stability behavior of the array. A quasi-steady stability analysis by Mureithi (1993) and Paidoussis et al. (1996) showed that a single flexible tube within a rotated triangle array in liquid flow is highly unstable. On the other hand, Mureithi's (1993) measured force field shows that a single flexible tube should remain stable if constrained to move only in the flow direction. This is confirmed above by the experimental results of Figs. 15–17 (one-tube flexible).

3.5. Stability behavior in two-phase flow

Preliminary test have recently been conducted in two-phase air–water flow on a rotated triangle array having $P/D = 1.5$. A brief summary of the test results is presented in this section. The reader is referred to Violette et al. (2005)

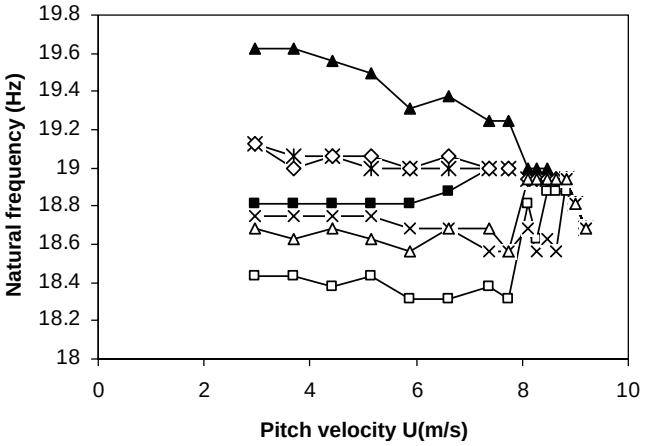

Fig. 19. Response frequency versus flow velocity for seven-flexible tube test: ■, tube 2; ∗, tube 3; ▲, tube 4; ◇, tube 5; □, tube 6; ×, tube 7; △, tube 8.

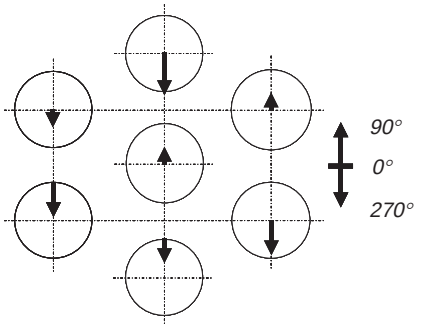

Fig. 20. The unstable mode for the seven-tube kernel.

for details. Tests have been conducted over a range of void fractions, corresponding to the mass-damping parameter range $2.5 < m\delta/\rho D^2 < 8$. Similar to the air-flow tests, no fluidelastic instability was observed for a single flexible cylinder. Furthermore, fluidelastic instability did occur for a seven-tube flexible kernel. Instabilities in two-phase flows were found to occur at significantly higher reduced flow velocities; thus, while a value of $K = 6.6$ is obtained in air-flow, the corresponding value is $K \approx 8$ in two-phase flow. The number of flexible tubes has a much more important effect in two-phase flow, indicating weakened coupling. Thus, a single flexible column of tubes remained stable in two-phase flow, while instability did occur in air-flow, albeit at significantly high flow rates ($K = 7.4$).

4. Discussion and conclusions

The series of tests presented in the foregoing is rather classical and in some sense, the results are not surprising. Fluidelastic instability is now known to be strongly dependent on coupling between neighboring tubes for its manifestation (Chen, 1983; Tanaka et al., 2002). It should come as no surprise that increased flexibility in the array results in reduced fluidelastic stability. This is well summarized in Fig. 21 where tube 2 response for different array flexibilities is replotted.

Table 2 presents a summary of the same results. Corresponding dimensionless parameters are also given. Notice that the resulting value of Connors constant $K = 5$ for the flexible bundle is well within the range of values obtained for axisymmetrically fully flexible tube bundles. This result is better reflected in the fluidelastic instability map of Fig. 22.

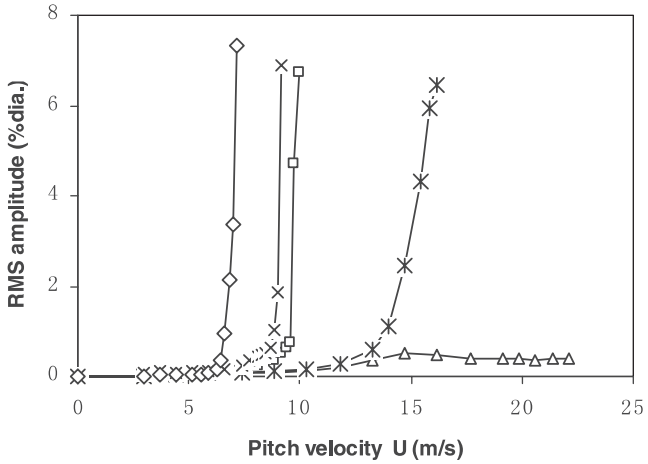

Fig. 21. Effect of array flexible on stability behavior (the response of tube 2 is shown in each case): △, one tube flexible; ∗, two tubes flexible; □, one column flexible; ×, seven tubes flexible; and ◇, all tubes flexible.

Table 2
Summary of fluidelastic instability results

	All tubes flexible	Seven tubes flexible	One column flexible	Two tubes flexible	One tube flexible
U_{pc}(m/s)	6.44	9.0	9.57	13.99	∞
U_{pc}/fD	8.4	12.5	12.5	18.3	∞
$2\pi m\zeta/\rho D^2$	2.82	3.59	2.87	2.37	2.18
K	5.0	6.6	7.4	11.9	∞

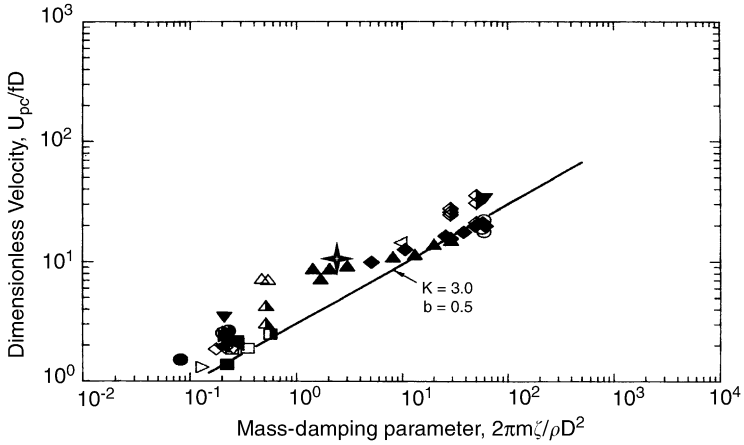

Fig. 22. Fluidelastic instability map for rotated triangular bundles: the present test for a flexible bundle (✦) is compared to previously reported tests on axisymmetrically flexible rotated triangle tube arrays; details of these tests may be found in Pettigrew and Taylor (1991) and references therein.

It is evident that the critical velocity for the fully axially flexible bundle measured here is within the same range of values found for arrays having axisymmetrically flexible tubes.

An important confirmation can be made from the present results. This is the fact that a single tube within a rotated triangular array cannot undergo single-degree-of-freedom fluidelastic instability in the flow direction. The reader is

reminded that the same array is highly unstable in cross-flow, even for the case of a single flexible cylinder (Weaver and Fitzpatrick, 1988; Mureithi et al., 1994). The cross-flow instability would be of less concern for an actual steam generator due to the fact that tubes would be supported in cross-flow by the AVBs. The same AVBs provide (on average) little support in the plane of the U-tubes, which corresponds to the inflow direction in the present work.

The question raised in the present work is whether the risk of instability in the in-flow direction exists.

Within a steam generator, a single flexible tube configuration would be the most likely to occur. Hence, it is the potential instability of a single flexible tube that raises most concern. The results presented here show that such an instability would not occur. Thus, an in-flow instability would require the unlikely event of having at least two adjacent tubes essentially unsupported at the same location. Even in this case, the instability velocity is still twice as high as that for the case of a fully flexible array of tubes. The preliminary two-phase flow test results briefly presented in the foregoing tend to indicate that the present air-flow test results may be conservative. Thus, in two-phase flow, significantly more than two flexible tubes may be needed for instability to occur at low enough flow velocities for concern.

References

Chen, S.S., 1983. Instability mechanisms and stability criteria of a group of circular cylinders subjected to cross-flow: Part 1 and 2. ASME Journal of Vibration, Stress and Reliability in Design 105, 51–58 and 253–260.

Fluit, S., Pettigrew, M.J., 2001. Simplified method for predicting vibration and fretting-wear in nuclear steam generators. ASME Publication PVP 420-1, Flow Induced Vibration. ASME, New York, pp. 7–16.

Mureithi, N.W., Price, S.J., Paidoussis, M.P., 1994. The post-hopf-bifurcation response of a loosely supported cylinder in an array subjected to cross-flow: Part I: experimental results. Journal of Fluids and Structures 8, 833–852.

Mureithi, N.W., 1993, Nonlinear dynamics of a loosely supported cylinder in cross-flow. Ph.D. Thesis, McGill University, Montreal, QC, Canada.

Pettigrew, M.J., Taylor, C.E., 1991. Fluidelastic instability of heat exchanger tube bundles: review and design recommendations. ASME Journal of Pressure Vessel Technology 113, 242–256.

Pettigrew, M.J., Taylor, C., 1994. Two-phase flow-induced vibration: an overview. ASME Journal of Pressure Vessel Technology 116, 233–253.

Pettigrew, M.J., Taylor, C., 2003. Vibration analysis of shell-and-tube heat exchangers: an overview, Part 1: flow, damping, fluidelastic instability; Part 2: vibration response, fretting wear, guidelines. Journal of Fluids and Structures 18, 469–500.

Païdoussis, M.P., 1983. A review of flow-induced vibrations in reactor and reactor components. Nuclear Engineering and Design 74, 31–60.

Païdoussis, M.P., Price, S.J., Mureithi, N.W., 1996. On the virtual nonexistence of multiple instability regions for some heat-exchanger arrays in cross-flow. ASME Journal of Fluids Engineering 118, 103–109.

Price, S.J., 1995. A review of theoretical models for fluid-elastic instability of cylinder arrays in cross-flow. Journal of Fluids and Structures 9, 463–518.

Tanaka, H., Tanaka, K., Shimizu, F., Takahara, S., 2002. Fluidelastic analysis of tube bundle vibration in cross-flow. Journal of Fluids and Structures 16, 93–112.

Violette, R., Mureithi, N.W., Pettigrew, M.J., 2005. Two-phase flow induced vibration of an array of tubes preferentially flexible in the flow direction. In: Pettigrew, M.J., Mureithi, N.W. (Eds.), Flow-Induced Vibration 2005. ASME, New York, paper No. PVP2005-71001.

Weaver, D.S., Fitzpatrick, J.A., 1988. A review of cross-flow induced vibrations in heat exchanger tube arrays. Journal of Fluids and Structures 2, 73–93.

Weaver, D.S., Schneider, W., 1983. The effect of flat bar supports on the cross flow induced response of heat exchanger U-tubes. ASME Journal of Engineering for Power 105, 775–781.

Weaver, D.S., Koroyannakis, D., 1983. Flow-induced vibrations of heat-exchanger U-tubes: a simulation to study the effects of asymmetric stiffness. ASME Journal of Vibration, Acoustics, Stress, and Reliability in Design 105, 67–75.